Available online at www.eccomasproceedia.org
Eccomas Proceedia COMPDYN (2025) 6004-6011

ECCOMAS
Proceedia

COMPDYN 2025
10th ECCOMAS Thematic Conference on
Computational Methods in Structural Dynamics and Earthquake Engineering
M. Papadrakakis, M. Fragiadakis (eds.)
Rhodes Island, Greece, 15-18 June 2025

EVALUATION OF THE SEISMIC HAZARD IN THE EASTERN MEDITERRANEAN REGION

Z. Cagnan[1]

[1] Engineering Sciences Department, Faculty of Engineering, Middle East Technical University, Dumlupinar Bulvari, Universiteler Mahallesi, Ankara, Turkey, 06800
e-mail: zehrae@metu.edu.tr

Abstract

The potential domino effect of the M_w7.8 Pazarcik earthquake in Turkey on the Dead Sea Fault and the Cyprus Fault has been extensively discussed in the literature (e.g., [1]; [2]; [3]). This study utilizes recent findings and outputs from various research projects on seismicity and fault characterization in the Eastern Mediterranean region to develop an updated regional seismic hazard model.

I incorporate alternative earthquake recurrence models along with recently derived global and regional ground motion prediction models into the current seismic hazard model. A probabilistic seismic hazard assessment is conducted based on a fault source model capable of generating large-magnitude earthquakes, as well as a smoothed seismicity model for background small-magnitude events.

The results of the time-independent and time-dependent seismic hazard assessment are presented in terms of the spatial distributions of three ground motion intensity measures: peak ground acceleration, 0.2 s and 1 s spectral accelerations, for site conditions with V_{s30} of 800 m/s, featuring a 475-year return period and a 2500-year return period. Additionally, hazard curves for selected cities are provided and compared with results from previous studies.

Keywords: Cyprus Arc, Subduction Zone, East Mediterranean, Seismic Hazard Assessment.

ISSN:2623-3347 © 2025 The Authors. Published by Eccomas Proceedia.
Peer-review under responsibility of the organizing committee of COMPDYN 2025.
doi: 10.7712/120125.12866.25274

1 INTRODUCTION

The East Anatolian Fault Zone constitutes one of the principal active strike-slip fault zones within the Eastern Mediterranean region, facilitating the deformation between the Anatolian Block and the Arabian Plate. On February 6, 2023, the East Anatolian Fault Zone experienced reactivation due to the moment magnitude (M_w) 7.8 Kahramanmaraş Earthquake, which produced a surface rupture approximately 375 kilometers in length, extending from the northeast of Çelikhan in the north to the Amik Basin in the south [4]. The earthquake originated on the Narli fault, subsequently triggering the main trace of the East Anatolian Fault Zone. Analysis of the southernmost segment of the Kahramanmaraş earthquake rupture reveals a releasing stepover of approximately 10.5 kilometers in width, situated between the southern terminus of the rupture and the northernmost segment of the Dead Sea Fault Zone. The Dead Sea Fault Zone is characterized by simple geometry in the south; however, it diverges into multiple branches as it progresses northward. This area encompasses the Hatay Triple Junction, which symbolizes a complex plate boundary fault configuration involving the relative motions of the African, Arabian, and Anatolian plates. These movements are accommodated by the strike-slip East Anatolian Fault Zone, the Dead Sea Fault Zone, and the reverse Larnaka-Amanos Fault Zone, which converge at the Hatay Triple Junction.

A notable phenomenon observed in the seismic behavior along major active fault zones is the domino-style triggering of large-magnitude earthquakes in adjacent segments, attributed to Coulomb stress transfer ([5], [6]). The Coulomb stress transfer models formulated by [7], [3], and [2] indicate significant stress loading on the neighboring segments of the Dead Sea Fault Zone and Larnaka-Amanos Fault Zone. Furthermore, the prolonged period of seismic quiescence observed along the Dead Sea Fault Zone, Larnaka-Amanos Fault Zone, and the Cyprus Arc- illustrated by the rupture of the Hacipaşa segment of the Dead Sea Fault Zone in 1408, by the rupture of the Larnaka-Amanos Fault Zone in 1961, by the rupture of the Eastern segment of the Cyprus Arc in 1993 - heightens the level of concern regarding expected seismic activity.

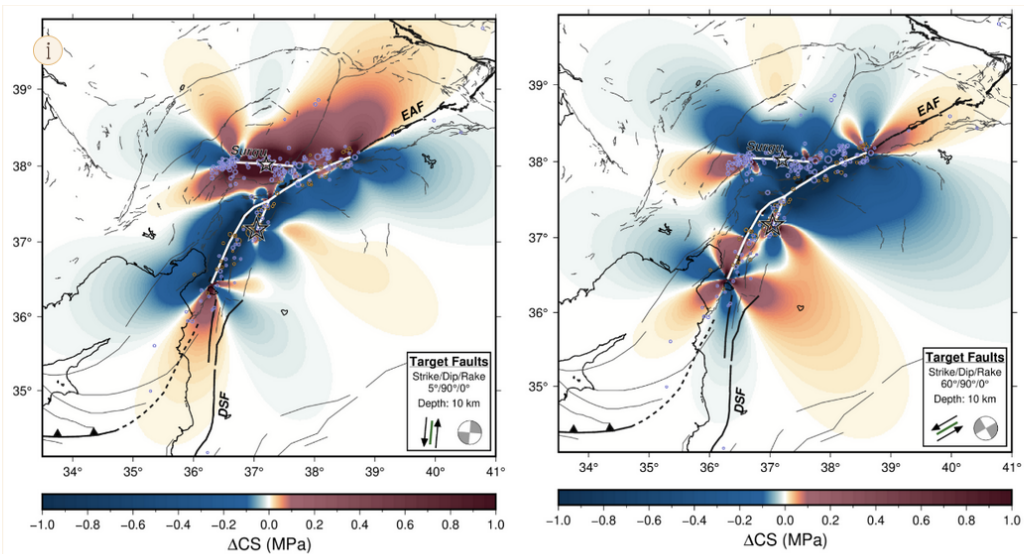

Figure 1: Coulomb stress transfer model developed by [7] based on the complete rupture observed from remote sensing for both 06.02.2023 M_w 7.8 and M_w 7.7 earthquakes of Turkey. The Figure on the left shows the Coulomb stress change on the Dead Sea Fault Zone and the Figure on the right shows the Coulomb stress change on the East Anatolian Fault Zone.

Cyprus is situated in a tectonically complex region at the boundary between the African and Eurasian tectonic plates, making it a seismically active area. The island is influenced by the subduction process of the African plate beneath the Eurasian plate alongside the Hellenic Arc to the west and the Cyprus Arc to the south. This tectonic convergence results in frequent seismic activity, characterized by moderate to strong earthquakes. The principal fault systems affecting Cyprus include the Paphos Transform Fault Zone and the Girne-Misis Fault Zone, which have been accountable for considerable historical seismic events. The majority of seismic activity is concentrated along the southern coastline and adjacent offshore regions, where active thrusting and strike-slip faulting are prevalent.

Tectonically, Cyprus is part of the Anatolian microplate, which is moving westward due to the collision between the Arabian and Eurasian plates. This movement influences faulting patterns across the island, resulting in both compressional and extensional stress regimes. The Troodos Ophiolite, a significant geological feature of Cyprus, is a remnant of the oceanic crust that was uplifted due to complex tectonic processes in the region. Although most earthquakes around Cyprus occur offshore, they can still pose risks to the island, as evidenced by historical seismic events that have caused damage to infrastructure and loss of life.

2 EARTHQUAKE RECCURENCE

In this study, a probabilistic seismic hazard assessment (PSHA) was conducted utilizing the fault source model and smoothed seismicity source model parameters derived from the European Seismic Hazard Model 2020 (ESHM 20) [8], as detailed in Tables 1-3. To encapsulate the epistemic uncertainty, the logic trees presented in Figures 2 and 3 were employed. A singular b value applicable to the tectonic region was utilized in conjunction with three distinct slip rate values and M_{max} values. The weights allocated to the branches that delineate slip rate uncertainty and those that denote M_{max} uncertainty are directly inherited from the study identified as ESHM 2020. In the aforementioned study, long- term geological or geodetic slip rates were converted into activity rates based on the premise of seismic moment conservation. The maximum magnitudes associated with the fault sources under consideration were estimated according to [9]' s fault scaling law. It was posited that the uncertainties associated with the maximum magnitude and slip rate parameters were correlated [10]. In articulating the shallow crustal earthquake productivity of active faults, the ESHM 20 employs spatially symmetric buffer zones in alignment with the top trace of the fault. Specifically, in the case of the East Anatolian Fault Zone, Antakya fault, and segments 1 and 4 of the Dead Sea Fault Zone, the occurrence rates of events with magnitudes $M_w \leq 6.7$ are represented by point sources located within the buffer zones. Conversely, the occurrence of events with magnitudes $M_w > 6.7$ is characterized as the earthquake productivity of the faults. For the remaining fault sources, the occurrence rates of magnitudes $M_w \leq M_{maxlower}$ - 0.6 are depicted by point sources situated within buffer zones, whereas events with magnitudes $M_w > M_{maxlower}$ - 0.6 are similarly defined as the earthquake productivity of these faults. This study employed the composite cumulative annual rates of both the active faults and point sources located within delineated buffer zones surrounding active faults.

In the present study, the Truncated Exponential model, as proposed by [11], along with the characteristic model, were employed as the earthquake recurrence models. The minimum event magnitude value selected for this analysis was 4.0. Furthermore, the Probabilistic Seismic Hazard Assessment (PSHA) was conducted utilizing the OpenQuake platform.

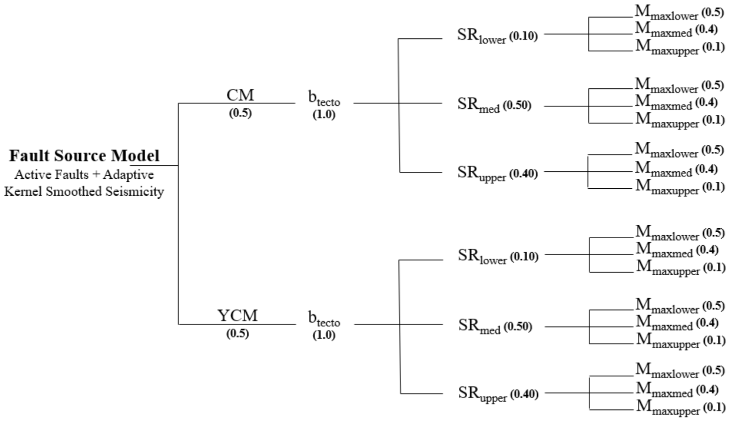

Figure 2: The adopted logic tree of the seismic sources for shallow crustal earthquakes in the PSHA. YCM stands for truncated exponential Youngs and Coppersmith earthquake recurrence model. CM stands for characteristic earthquake recurrence model. SR stands for slip rate, b_{tecto} stands for single b value representing the tectonic region, and M_{max} is the maximum magnitude assigned to the fault source. The subscripts lower, med, upper represent the lower bound, median, and upper bound values for the inputs, respectively.

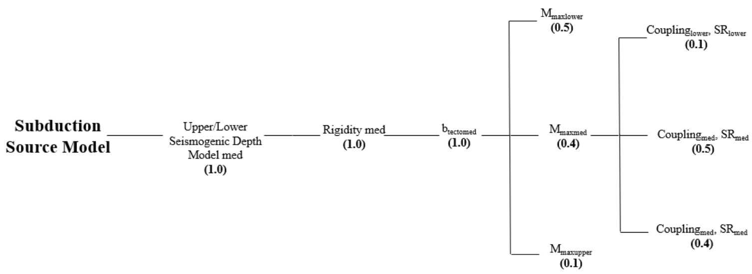

Figure 3: The adopted logic tree of the seismic sources for subduction earthquakes in the PSHA. SR stands for slip rate, b_{tecto} stands for single b value representing the tectonic region, and M_{max} is the maximum magnitude assigned to the fault source. The subscripts lower, med, upper represent the lower bound, median, and upper bound values for the inputs, respectively.

Fault Source Name	Fault ID	M_{max}			b_{tecto}	Slip rate (mm/year)		
		$M_{maxlower}$	M_{maxmed}	$M_{maxupper}$		SR_{lower}	SR_{med}	SR_{upper}
East Anatolian Fault Zone	TRCF002	8.1	8.5	9.1	0.978	5.40	7.15	8.90
Antakya Fault	TRCF00N	7.3	7.7	8.1	0.978	1.00	2.71	4.42
Larnaka-Amanos Fault Zone	CYCF000	7.1	7.5	7.5	0.898	0.19	0.85	1.50
Cyprus Arc	CYCF001	7.1	7.5	7.5	0.898	0.14	0.82	1.50
Pentakomo Fault	CYCF002	7.1	7.5	7.5	0.898	0.14	0.82	1.50
Paphos Transform	CYCF003	6.7	7.1	7.4	0.898	2.00	6.00	10.0

Fault Zone								
Girne-Misis Fault Zone	CYCF004	6.9	7.3	7.4	0.898	0.36	1.68	3.00
Larnaka-Amanos Fault Zone	SYCF000	6.9	7.3	7.4	0.898	0.19	0.85	1.50
Dead Sea Fault Zone	SYCF001	7.3	7.7	8.1	0.978	2.35	2.60	2.85
Dead Sea Fault Zone	SYCF002	7.1	7.5	8.1	0.978	3.00	5.00	7.00
Dead Sea Fault Zone	SYCF003	6.9	7.3	8.0	0.978	0.50	1.00	1.50
Dead Sea Fault Zone	SYCF004	7.3	7.7	8.1	0.978	1.39	2.82	4.25

Table 1: The fault source parameters as suggested by the source model of the ESHM20 European Seismic Hazard Model [8]. SR stands for slip rate, b_{tecto} stands for single b value representing the tectonic region, and M_{max} is the maximum magnitude assigned to the fault source. The subscripts lower, med, upper represent the lower bound, median, and upper bound values for the inputs, respectively.

Fault Source Name	Fault ID	M_{max}			b_{tecto}			Slip rate (mm/year)		
		$M_{maxlower}$	M_{maxmed}	$M_{maxupper}$	$b_{tectolower}$	$b_{tectomed}$	$b_{tectoupper}$	SR_{lower}	SR_{med}	SR_{upper}
Cyprus Arc Interface and Intra-slab Sources	CYSD001	8.1	8.4	8.7	1.05	1.07	1.15	9.76	12.2	14.6

Table 2: The fault source parameters of the Cyprus Arc Subduction Zone as suggested by the source model of the ESHM20 European Seismic Hazard Model [8]. SR stands for slip rate, b_{tecto} stands for single b value representing the tectonic region, and M_{max} is the maximum magnitude assigned to the fault source. The subscripts lower, med, upper represent the lower bound, median, and upper bound values for the inputs, respectively.

Source Name	Source ID	M_{max}	b_{tecto}	a_{tecto}	
Smoothed Seismicity	SZ25	7.1	0.898	3.95	5.10

Table 3: The smoothed seismicity as suggested by the source model of the ESHM20 European Seismic Hazard Model [8]. b_{tecto} stands for single b value representing the tectonic region, a_{tecto} stands for single a value representing the tectonic region, and M_{max} is the maximum magnitude assigned to the fault source. The subscripts lower, med, upper represent the lower bound, median, and upper bound values for the inputs, respectively.

3 GROUND MOTION ATTENUATION

In the case of shallow crustal earthquakes, the ground motion attenuation is modeled using the recent partially nonergodic ground motion prediction model developed by [12] for the Euro-Mediterranean region. In the case of deep events, the ground motion attenuation is modeled using the four recently developed global ground motion prediction models for interface and intra-slab events: [13], [14], [15] and [16]. Equal weights were assigned to these models in the PSHA carried out.

There are 435 three component ground motion records in hand for Cyprus. These represent the ground motion originating from shallow crustal events mainly. These records were mainly obtained at NEHRP C and D type sites. They correspond to M_w<5.5 events with source to site distances less than 120km. These records were utilized to study the regional attenuation and source characteristics of the Eastern Mediterranean region.

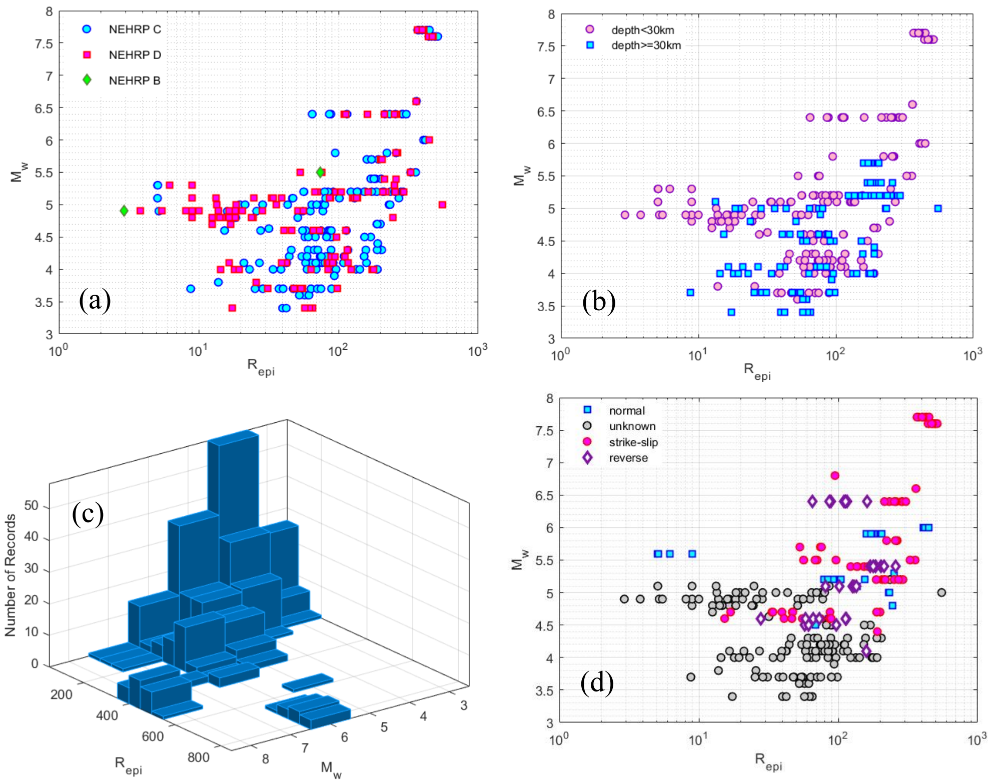

Figure 4: (a) Epicentral distance against moment magnitude distribution of ground motion records obtained from Eastern Mediterranean region as classified according to different site conditions, (b) epicentral distance against moment magnitude distribution of ground motion records obtained from Eastern Mediterranean region as classified according to depth of the epicentral location, (c) bar chart illustrating distribution of number of records with moment magnitude of associated events and source-to-site distance of station sites, (d) epicentral distance against moment magnitude distribution of ground motion records obtained from Eastern Mediterranean region as classified according to focal mechanism of causal events.

4 CONCLUSIONS

This research employs recent findings and outputs derived from various investigative endeavors pertaining to seismicity, fault characterization, and ground motion attenuation in the Eastern Mediterranean region, with the aim of formulating an updated regional seismic hazard model. The assessment of seismic hazard, both time-independent and time-dependent, yields results concerning the spatial distributions of three ground motion intensity measures: peak ground acceleration, 0.2-second spectral acceleration, and 1-second spectral acceleration, specifically for site conditions characterized by an average shear-wave velocity for the top 30 meters (V_{s30}) of 800 m/s. These measures are calculated for both a 475-year and a 2500-year return period and are critically compared with results obtained from previous studies.

REFERENCES

[1] E. Altunel, O. Kozaci, C. Yildirim, R. Sbeinati, M. Meghraoui, Potential of 20th Century North Anatolian Fault Style Domino Effect of the February 6, 2023, Kahramanmaraş Earthquake on the Centuries Long Dead Sea fault Seismic Quiescence. *Research Square*, 2024.

[2] S. Ergintav, P. Vernant, O. Tan, H. Karabulut, S.Ozarpacı, M. Floyd, A.O. Konca, Z. Cakir, D. Acarel, R. Cakmak, H.Vasyura-Bathke, U. Dogan, A.İ. Kurt, A. Ozdemir, E.T. Ayruk, M. Turgut, O. Ozel, İ Farımaz, Unexpected far-field deformation of the 2023 Kahramanmaraş Earthquakes Revealed by Space Geodesy. *Science*, 386, pp.328-335, 2024.

[3] G. Tanircan, T.K. Eken (Eds), Kandilli Observatory and Earthquake Research Institute Preliminary Earthquake Report on 6 Feburary 2023 Mw 7.7 Gaziantep, 6 February 2023 Mw 7.6 Kahramanmaraş, 20 February 2023 Mw 6.4 Hatay Earthquakes.Kandilli Observatory and Earthquake Research Institute, Bogazici University, 13 March, 2023.

[4] O. Kozaci, E. Altunel, R. Koehler, C. Yildirim, K. Clahan, M_W7.8 Kahramanmaras Earthquake Surface Fault Rupture and Near-Fault Effect Observations, Soils and Foundations 8th ICEGE Special Issue.

[5] Nalbant, S. S., McCloskey, J., Steacy, S. and Barka, A. A. 2002. Stress accumulation and increased seismic risk in eastern Turkey. Earth Planet Sci Lett. 195(3–4):291–298. doi:10.1016/S0012-821X(01)00592-1.

[6] Stein, R.S., Barka, A.A. and Dieterich, J.H., 1997. Progressive failure on the North Anatolian faultsince 1939 by earthquake stress triggering. Geophys. J. Int., 128, 594–604.

[7] R. Schmitt, M. Herman, W. Barnhart, K. Furlong, H. Benz, The 2023 Kahramanmaras, Turkey, Earthquake Sequence, U. S. Geological Survey Story Map, March 27, 2023.

[8] Danciu, L. et al., 2021. The 2020 update of the European Seismic Hazar Model ESHM20: model overview, EFEHR Technical Report 1.

[9] Leonard, M. 2014. Self-consistent earthquake faulting scaling relations: update and extension to stable continental strike-slip faults, Bulletin of the Seismological Society of America, vol.104, no.6, pp.2953-2965.

[10] Danciu et al., 2024. The 2020 European Seismic Hazard Model: Overview and Results, https://doi.org/10.5194/egusphere-2023-3062.

[11] Youngs, R.R. and K.J. Coppersmith 1985. Implications of fault slip rates and earthquake recurrence models to probabilistic seismic hazard estimates, Bulletin of the Seismological Society of America, vol.75, issue:4, pp.939-964.

[12] Kotha et al. 2022. Near-source magnitude scaling of spectral accelerations: analysis and update of Kotha et al. (2020) model, Bulletin of Earthquake Engineering, vol.20, pp.1343-1370.

[13] Abrahamson, N., and Z., Gülerce 2021. Summary of the Abrahamson and Gulerce NGA-SUB ground-motion model for subduction earthquakes, Earthquake Spectra, vol. 38, issue:4, pp.2638-2681.

[14] Kuehn et al., 2021. Partially non-ergodic ground motion model for subduction regions using NGA-Subduction database, Earthquake Spectra, vol.39, issue:3, pp.1625-1657.

[15] Parker et al., 2021. NGA-Subduction global ground motion models with regional adjustment factors, Earthquake Spectra, vol.38, issue:1, pp.456-493.

[16] Si et al., 2020. Development of NGA-sub ground motion model of 5% damped pseudo-spectral acceleration based on database for subduction earthquakes in Japan. PEER Report. Berkeley, CA: Pacific Earthquake Engineering Research Center, University of California, Berkeley.